Rare Metal Materials and Engineering
Volume 52, Issue 6, June 2023
Available online at www.rmme.ac.cn

Science Press

Cite this article as: Shi Zhenxue, Liu Shizhong, Yue Xiaodai, et al. Effect of Re Content on Mircrostructure and Stress Rupture Properties of DD15 Single Crystal Superalloy[J]. Rare Metal Materials and Engineering, 2023, 52(06): 1977-1984.

ARTICLE

Effect of Re Content on Mircrostructure and Stress Rupture Properties of DD15 Single Crystal Superalloy

Shi Zhenxue, Liu Shizhong, Yue Xiaodai, Wang Zhicheng, Li Jiarong

Science and Technology on Advanced High Temperature Structural Materials Laboratory, Beijing Institute of Aeronautical Materials, Beijing 100095, China

Abstract: The fourth generation single crystal superalloy DD15 with Re content of 5wt%, 6wt%, and 7wt% was cast in the directionally solidified furnace, while other alloying elements were basically the same in content. The long term aging after full heat treatment was performed at 1100 °C for 1000 h. The stress rupture tests of the alloy were conducted under 1100 °C/137 MPa. The effect of Re content on the microstructure and stress rupture properties of the alloy was investigated. The results show that the size of γ' phase decreases, the volume fraction and cubic degree of γ' phase slightly increase with increase in Re content. After long term aging, the γ' phase coarsens, and the drafting rate, precipitate rate and volume fraction of TCP phase are all improved with increase in Re content. With the increase in Re content, the microstructure stability and the stress rupture life of the alloy decline significantly. The three ruptured specimens all exhibit the presence of TCP phase. The amount of TCP phases increases greatly with increase in Re content. TCP phase can be the site of crack initiation. This is the main reason for the decrease in stress rupture life of the alloy with increase in Re content. The dislocation networks formed at the γ/γ' interface of ruptured specimen turn denser with increase in Re content. Re has a strong segregation tendency in γ matrix. The partition ratio of Re rises significantly with increase in Re content. The lattice misfit of the alloy becomes larger toward negative with increase in Re content.

Key words: single crystal superalloy; DD15; Re content; stress rupture properties

The single crystal superalloy has been widely used as key material to manufacture the blade part of advanced aerospace turbine engines[1]. A lot of high melting point alloying elements are added to strengthen the alloy. The temperature capability of the alloy has been increased significantly in the past several decades. Re is a crucial alloying element in the single crystal superalloys. The first generation single crystal superalloys do not contain Re element. A certain amount of Re added to the single crystal superalloy can improve the temperature capability of the turbine blade. Re contents of 3% and 6% are the prominent features of the second and third generation single crystal superalloy, respectively[2]. Their temperature capability is 30 and 60 °C higher than that of the first generation alloys, respectively[3]. The Re addition significantly promotes the development and application of the single crystal superalloy.

Re element is found to be mainly distributed in the γ phase, in which it forms clusters with size of about 1 nm and mutual average distances of 20 nm[4–5]. Re can produce a large solution strengthening effect because of its large atom radius. The existence of Re cluster has a greater strengthening effect than the traditional solution method[6]. The lattice misfit of the alloy with Re addition is more negative, which has an effect roughly three times stronger than effect of tungsten addition on the γ/γ' misfit because rhenium nearly totally concentrates in the γ matrix while tungsten dissolves in both the γ and γ' phases[7]. The diffusion activation energy of Re in Ni is higher than that of other common alloying elements in Ni[8]. So the low diffusion coefficient of Re can slow down the coarsening of γ' phase[9–11]. Re segregates at dislocation core regions in the dislocation networks to greatly slow down inter-diffusion in the interface region and to retard dislocation motion at the γ/γ' interface[12–13]. Re-decorated dislocation networks along the phase boundaries act as mechanical walls that effectively

Received date: December 08, 2022
Foundation item: National Science and Technology Major Project (2017-VI-0002-0071, J2019-III-0008-0052)
Corresponding author: Shi Zhenxue, Ph. D., Professor, Science and Technology on Advanced High Temperature Structural Materials Laboratory, Beijing Institute of Aeronautical Materials, Beijing 100095, P. R. China, Tel: 0086-10-62498312, E-mail: zhenxue.shi@biam.ac.cn

Copyright © 2023, Northwest Institute for Nonferrous Metal Research. Published by Science Press. All rights reserved.

block dislocation motion and crack propagation[14]. A Re atom occupying either a Ni site in the γ phase or an Al site in the γ' phase can strongly enhance the bonding strength between Re and its nearest neighboring atoms, suggesting that the substitution atom Re will influence dislocation motion along the γ/γ' interface[15].

So Re can greatly improve the mechanical properties of the alloys[16–19]. Moreover, Re can lower the oxidation rate of the alloy[20]. Recrystallization is suppressed with the addition of Re because incubation period is prolonged and nucleation slows down[21]. However, the single crystal superalloy is easy to form topologically close-packed (TCP) phases and secondary reaction zone (SRZ) with increase in Re content[22–23]. Ru addition can restrain precipitation of TCP phases in the fourth generation single crystal superalloys[24–25]. The Re addition also strongly increases the amount of eutectic and the tendency for microsegregation[26].

Although the mechanism of Re action has been studied extensively, there are still different opinions, such as Re cluster[27] and the enrichment of Re at the γ/γ' interface[3]. The price of Re is very high. In order to lower the consumption of rhenium and to reduce the product cost, the research on effect and mechanism of Re doping is needed. Moreover, there are few studies on influencing mechanism of Re in high generation single crystal superalloys. The fourth generation single crystal superalloy DD15 was developed by Beijing Institute of Aeronautical Materials[16–17,28–29]. The chemical composition of DD15 alloy, including Re content, is obviously different from that of typical fourth generation alloys abroad, such as EPM-102[1], TMS-138[30], MC-NG[31]. In order to optimize the chemical composition, microstructure, overall performance and cost reduction of DD15 alloy, it is necessary to investigate the effect of Re content on microstructure and stress rupture properties of the alloy.

1 Experiment

Three single crystal samples with the size of Φ15 mm×180 mm were prepared using crystal selection method in the vacuum directional solidification furnace. The Re content of three alloys was 5wt%, 6wt%, 7wt% while keeping the other alloying element content the same. The nominal chemical compositions of three alloys are listed in Table 1. The crystal orientations of the samples were analyzed with X-ray diffraction instrument, and the growing orientation was within 15° deviating from the [001] orientation. The heat treatment of the samples was proceeded according to their heat treatment regime. All the samples were subjected to long term aging at 1100 °C for 200, 400, 600, 800 and 1000 h. The standard cylindrical specimens for stress rupture tests were machined after standard heat treatment. The stress rupture tests were conducted under 1100 °C/137 MPa in air. The microstructures of the alloys under different conditions were examined using scanning electron microscope (SEM) and transmission electron microscopy (TEM). Element distribution at γ/γ' interface of the alloy was measured by EDS attached to TEM. The lattice misfit was determined by high resolution X-ray diffraction method. The γ'/γ lattice misfits $\delta=2(a_{\gamma'}-a_{\gamma})/(a_{\gamma'}+a_{\gamma})$, where $a_{\gamma'}$ and a_{γ} are the lattice parameters of γ' phase and γ phase, respectively, and calculated from the experimental XRD patterns.

2 Results and Discussion

2.1 Microstructure after heat treatment

Fig. 1 shows the microstructure of the alloy samples with different Re contents after standard heat treatment. It can be seen that there are coherently embedded cubical γ' phase in γ matrix. The γ/γ' eutectic and coarse γ' phase are completely eliminated in the process of high temperature insulation. The new fine γ' phase precipitates from the supersatured γ solid solution coherently during the subsequent cooling process. The uniformly distributed cubic γ' phase is obtained after high temperature aging and low temperature aging treatment. Comparing Fig. 1a–1c, it can be seen that the size of γ' phase decreases and the cubic degree of γ' phase slightly increases with increase in Re content. Fig. 2 shows the effect of Re content on the size and volume fraction of γ' phase of the alloy calculated by data statistics. The γ' phase size is 200–400 nm and the volume fraction of γ' phase is 60%–70% for the alloy with different Re contents. It is shown that the size of γ' phase decreases and the volume fraction of γ' phase increases with increase in Re content.

2.2 Microstructure after long term aging

Fig. 3 illustrates the microstructure of the alloy damples with different Re contents after long term aging at 1100 °C. It can be seen that for the alloy containing 5wt% Re, the size of γ' phase turns bigger and its morphology is still in cubic shape after long term aging for 200 h. The adjacent γ' particles meet and fuse together to produce rafts along the [100] or [010] direction and no TCP phase is observed after long term aging for 800 h. A small amount of needle shaped TCP phase is precipitated at the angle of 45° relative to the rafting direction of γ' phase after long term aging for 1000 h. It indicates that the alloy with 5wt% Re has a good microstructure stability.

Most of γ' precipitates are still in cubic shape and there is no TCP phase observed after long term aging for 200 h in the alloy with 6wt% Re. The rafts fully form and a lot of needle shaped TCP phases are observed after long term aging for 400

Table 1 Nominal chemical compositions of experimental alloy samples (wt%)

Sample	Cr	Co	Mo	W	Ta	Re	Ru	Nb	Al	Hf	Ni
5%Re	2–4	7–10	0.8–1.5	6–9	7–10	5	2–4	0.2–1.0	5–6	0.1–0.3	Bal.
6%Re	2–4	7–10	0.8–1.5	6–9	7–10	6	2–4	0.2–1.0	5–6	0.1–0.3	Bal.
7%Re	2–4	7–10	0.8–1.5	6–9	7–10	7	2–4	0.2–1.0	5–6	0.1–0.3	Bal.

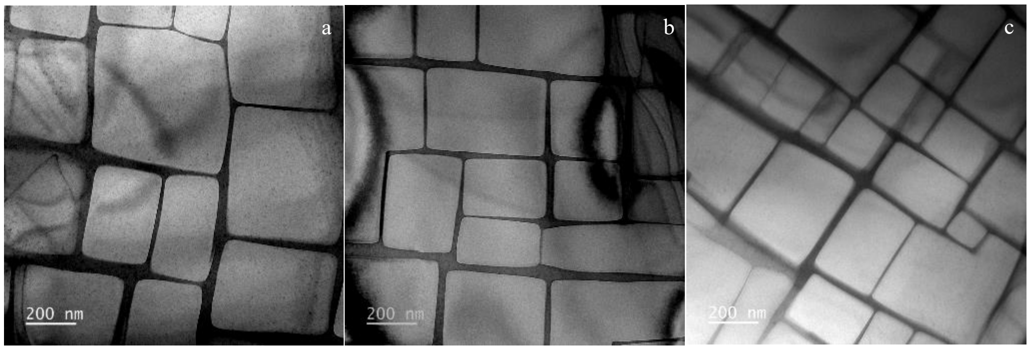

Fig.1 Microstructures of the alloy samples with different Re contents after standard heat treatment: (a) 5wt%, (b) 6wt%, and (c) 7wt%

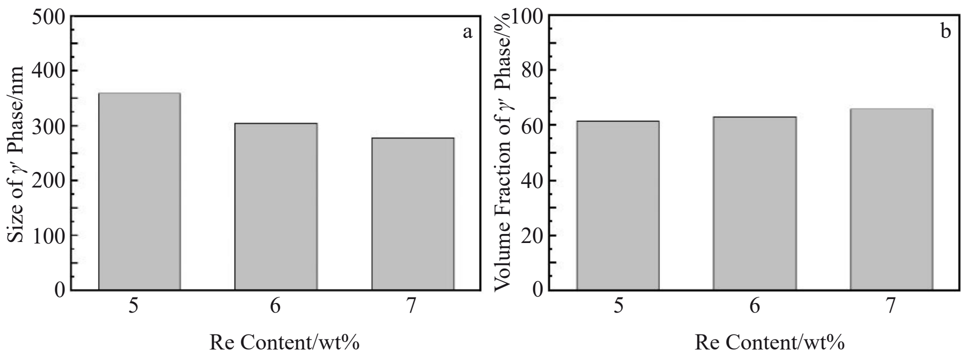

Fig.2 Effect of Re content on size (a) and volume fraction (b) of γ' phase for the alloy samples

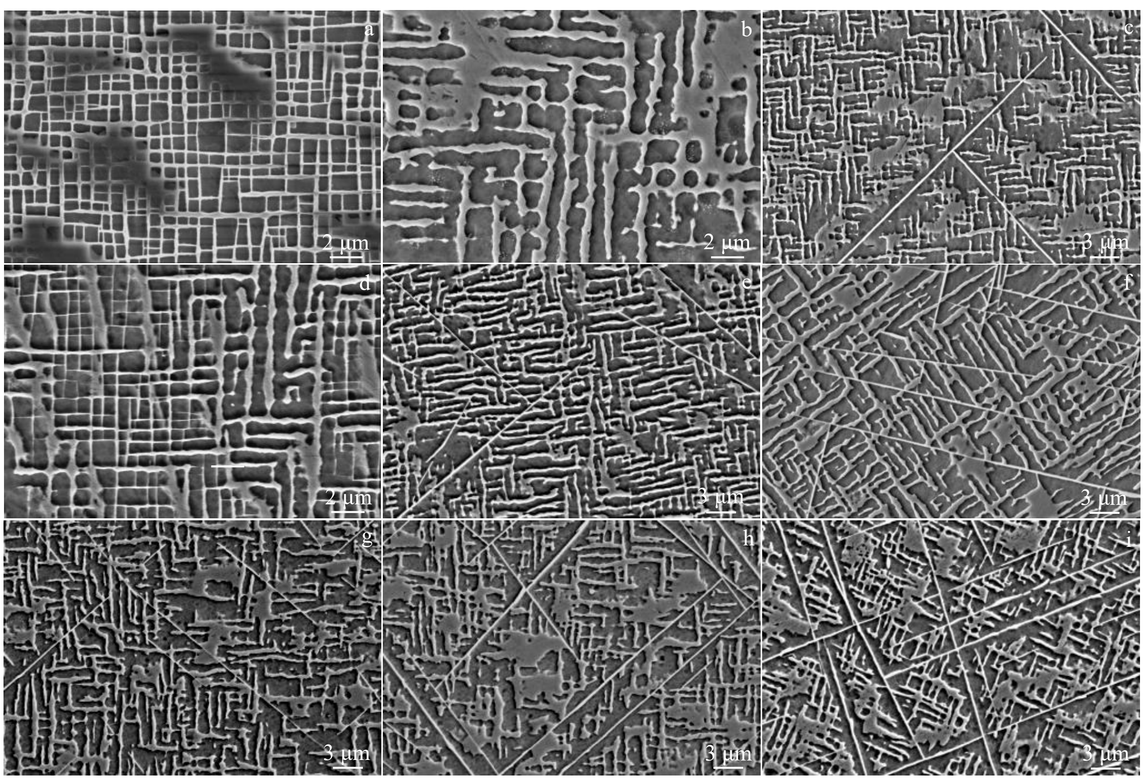

Fig.3 Microstructures of the alloy samples with different Re contents after long term aging at 1100 °C for different time: (a) 200 h, 5wt% Re; (b) 800 h, 5wt% Re; (c) 1000 h, 5wt% Re; (d) 200 h, 6wt% Re; (e) 400 h, 6wt% Re; (f) 1000 h, 6wt% Re; (g) 200 h, 7wt% Re; (h) 400 h, 7wt% Re; (i) 1000 h, 7wt% Re

h. The amount of TCP phase increases significantly after long term aging for 1000 h.

The rafting structure forms and there is a lot of TCP phase observed after long term aging for 200 h in the alloy with 7wt% Re. The amount of TCP phase increases significantly after long term aging for 400 and 1000 h.

Comparing the long term aging microstructure of the alloy with different Re contents, the conclusion can be drawn that the γ' phase coarsening and drafting rate, the precipitate rate and volume fraction of TCP phase are all improved with increase in Re content. So the microstructure stability of the alloy declines with increase in Re content.

The chemical composition of TCP phases in the alloy with different Re contents after aging at 1100 °C for 1000 h is shown in Table 2. In three specimens, Re, W, Co, Ta is enriched in the TCP phases. In contrast, the content of Re and W in the TCP phase becomes higher with increase in Re content.

2.3 Stress rupture properties

The stress rupture properties of the alloys with different Re contents under 1100 °C/137 MPa are shown in Fig.4. It can be seen that the stress rupture life of the alloy reduces and the elongation decreases at first and then decreases with increase in Re content. As Re content of the alloy increases from 5wt% to 6wt% and to 7wt%, the stress rupture life is decreased by 9% and 22%, respectively. It indicates that increasing Re content can significantly reduce the stress rupture life of the alloy at high temperatures.

Table 2 Chemical composition of TCP phase in three alloys after aging at 1100 °C for 1000 h (wt%)

Sample	Al	Cr	Co	Ta	Ru	W	Re	Mo	Ni
5%Re	4.5	2.2	7.2	6.8	2.3	13.4	16.6	1.4	Bal.
6%Re	2.9	2.4	6.1	6.3	2.5	16.1	18.5	2.6	Bal.
7%Re	2.4	2.7	6.4	4.3	2.4	17.2	30.6	2.2	Bal.

2.4 Microstructure of stress ruptured specimens

The microstructure of the longitudinal section of the ruptured specimens under 1100 °C/137 MPa was observed by SEM. Fig.5 and Fig.6 illustrate the microstructures apart from 1.5 cm to fracture surface and region near fracture surface of the ruptured specimens, respectively. It can be seen in Fig. 5 that the γ' particles transform into the rafted structure along the direction perpendicular to the stress axis for three alloys. There is no significant difference in the thickness of raft with increase in Re content. Fig.6 shows that the γ phase is no longer continuous, forming islands that are entirely surrounded by the γ' phase, which is called "topological inversion"[32]. The three ruptured specimens all exhibit the presence of TCP phase. The amount of TCP phases increases greatly with increasing Re content. It indicates that increasing Re content can reduce high temperature microstructure stability of the alloy. This is in good agreement with the result of the long term aging experiment. The cracks form in alloys with 6wt% and 7wt% Re. TCP phase is brittle and becomes the site of crack initiation. The cracks increase and become bigger with increasing Re content. Therefore, this is the main reason why the stress rupture life of the alloy decreases with increase in Re content.

Fig. 7 shows the morphologies of γ/γ' interfacial dislocation

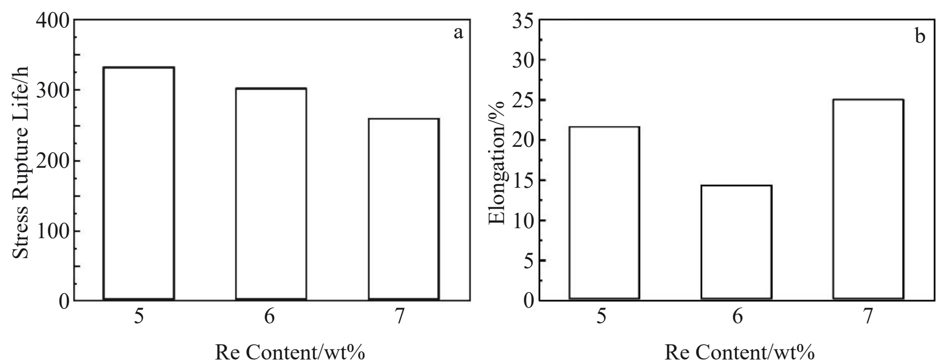

Fig.4 Influence of Re content on the stress rupture life (a) and elongation (b) of the alloy samples

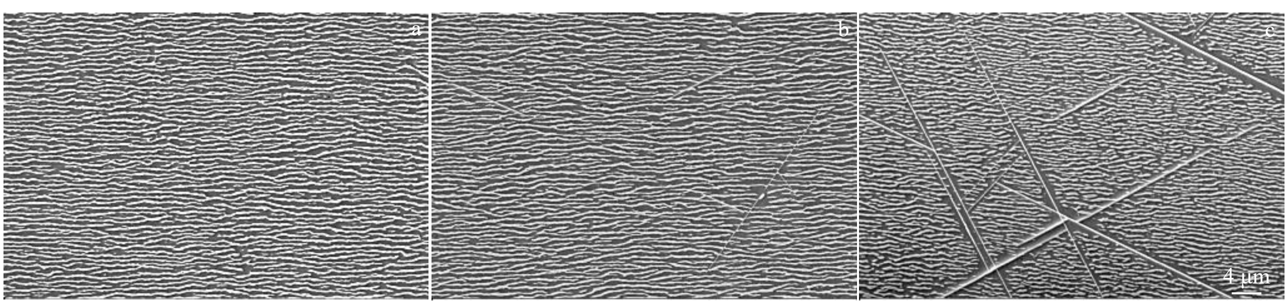

Fig.5 Microstructures apart from 1.5 cm to fracture surface of ruptured samples under 1100 °C/137 MPa: (a) 5%Re, (b) 6%Re, and (c) 7%Re

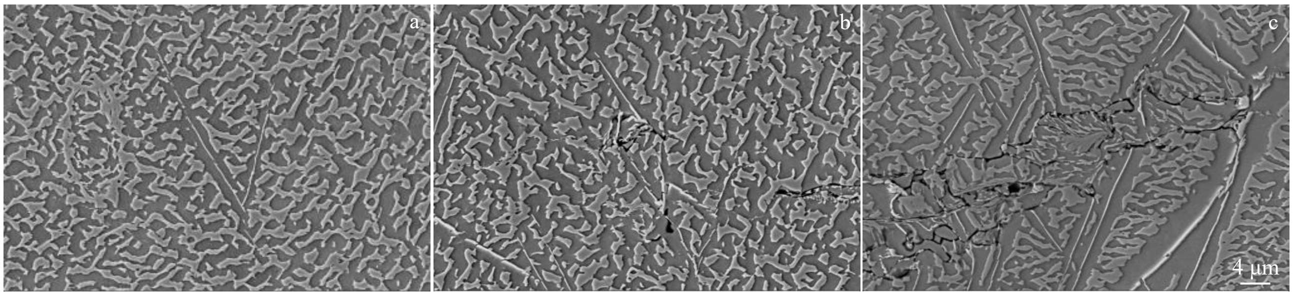

Fig.6 Microstructures near the fracture surface of ruptured samples under 1100 °C/137 MPa: (a) 5%Re, (b) 6%Re, and (c) 7%Re

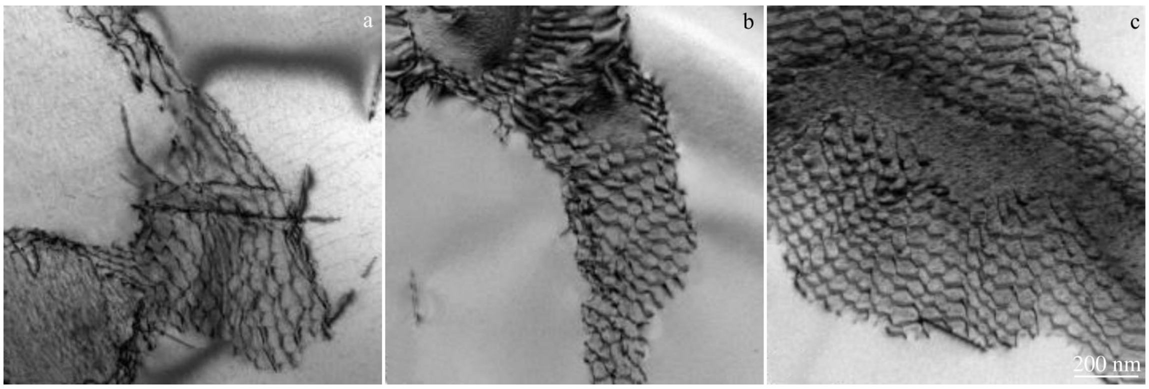

Fig.7 TEM images of ruptured samples under 1100 °C/137 MPa: (a) 5%Re, (b) 6%Re, and (c) 7%Re

of stress ruptured specimens under 1100 °C/137 MPa. The dislocation networks form at the *γ*/*γ*′ interface due to the reaction of dislocation with different Burgers vectors. It clearly shows that the dislocation network of the alloy turns denser and much more better with increase in Re content. The dense *γ*/*γ*′ interfacial dislocation network will effectively prevent the dislocation from cutting into *γ*′ phase in the creep process[25,33]. The lattice misfit of the alloy is more negative with increase in Re content. The denser *γ*/*γ*′ interfacial dislocation networks make the alloy maintain a minimum creep rate in the steady state stage.

3 Discussion

3.1 Element distribution

Element distribution at *γ*/*γ*′ interface of the alloy was measured by EDS attached to TEM. Elemental profile at the *γ*/*γ*′ interface of the alloy with different Re contents is shown in Fig. 8. The comparison of the partition ratio of alloying element in the two alloys is shown in Fig.9. The partition ratio is given by $k_i=C_i^{\gamma}/C_i^{\gamma'}$, where *i* corresponds to a particular element, and C_i^{γ} and $C_i^{\gamma'}$ correspond to the concentration of alloying element *i* in the *γ* and *γ*′ phases, respectively. It can be seen from Fig.8 and Fig.9 that the distribution behavior of the same element in *γ* matrix and *γ*′ phase is similar in the alloy with 5% and 7% Re. There is no evidence for the enrichment of Re at the *γ*/*γ*′ interface. Comparing chemical composition of *γ*′ phases and *γ* matrix, it can be seen that the *γ*′ phases are highly enriched with Al and Ta, while the *γ* matrix contains characteristically elevated levels of Re, Ru, W, Co, Cr and Mo. The partition ratio of Re, Ta, Mo, Cr Al increases and that of W, Ru, Co decreases with increase in Re content. Among

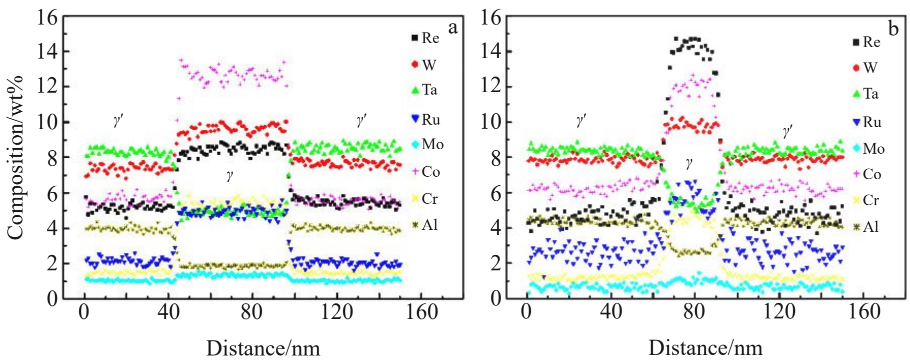

Fig.8 Elemental profile at the *γ*/*γ*′ interface for the alloy samples with 5wt% (a) and 7wt% (b) Re

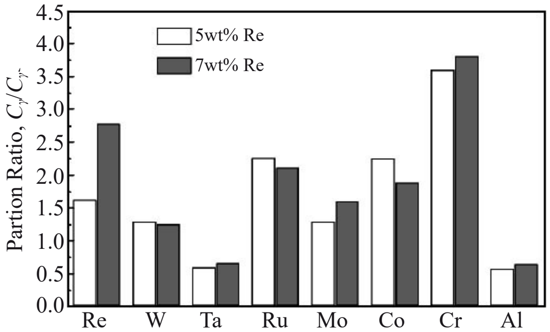

Fig.9 Partition ratio of element in the alloy samples with 5wt% and 7wt% Re

these elements, Re has a strong segregation tendency in γ matrix. Moreover, the partition ratio of Re rises significantly with increase in Re content.

The microstructure stability at elevated temperatures is a key concern for the high generation single crystal superalloys[24]. The formation of TCP phases in Ni-based single crystal superalloys is generally attributed to the supersaturation of high melting point refractory elements within the disordered γ phase[34]. Therefore, the saturation degrees of Re, Ta, Mo in the γ matrix increase, which makes it easy for the formation of TCP phases in 7%Re alloy at high temperature. It indicates that the microstructure stability at high temperature of the alloy declines with increase in Re content.

3.2 Lattice misfit

It is known that γ/γ' lattice misfit influences the morphology of γ' phase, mechanical properties and phase stability of single crystal superalloys[35]. The γ'/γ lattice misfit is calculated from the experimental XRD patterns. Comparison of XRD patterns for alloys with different Re contents is shown in Fig. 10. By analysis and calculation, the lattice misfit of alloy sample with 5wt% Re and 7wt% Re is –0.08 and –0.19, respectively. The lattice misfit of the alloy turns larger toward negative with increase in Re content because of higher amounts of Re that preferentially part the γ phase and expand the lattice parameter of γ phase.

γ' phase is spherical in alloys with a near zero misfit, whereas it becomes cuboidal when the lattice misfit deviates from zero in either the positive or negative direction[36]. So the cubic degree of γ' phase slightly increases with increase in Re content because the lattice misfit of the alloy turns larger toward negative. The coherency stress between γ and γ' phases induced by the lattice misfit is reported to increase the kinetics of γ' coarsening and rafting during unstressed long term aging[37]. Long term aging experiment shows that the coarsening and drafting rates of γ' phase are improved with increase in Re content.

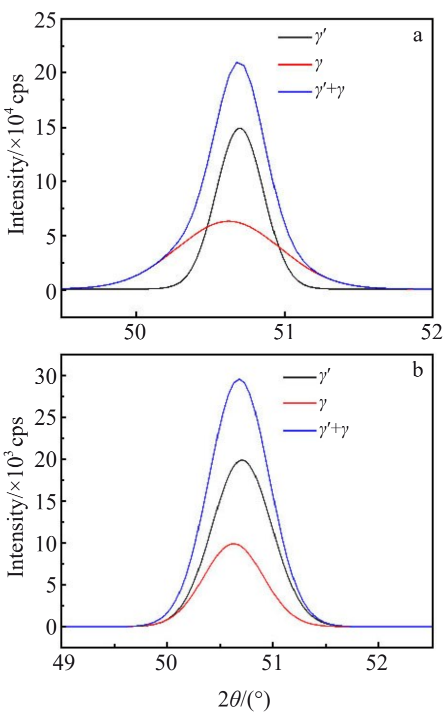

Fig.10 XRD patterns of alloy samples with 5wt% Re (a) and 7wt% Re (b)

3.3 Stress rupture properties

Re element plays an important role in improving the temperature capability of the high generation single crystal superalloy[13–19]. A significant characteristic is that Re has the slowest diffusion rate in nickel. The solid solution strengthening effect of the alloy is enhanced with increase in Re content. The lattice misfit is the driving force for the rafting behavior during creep deformation and is known to enhance the creep property at high temperature and low stress[38]. In addition, the denser dislocation networks resulted from increasing Re content can effectively prevent the subsequent dislocation from cutting into γ' precipitate and make the alloy maintain a minimum creep rate[25,33]. However, the above beneficial effect of Re is not offset by the adverse factor of significant increase in TCP phase precipitation. It can be seen from Fig. 6 that the crack initiates and propagates in the TCP phase, and the microcracks disrupt the rafted γ' precipitates.

There are some reasons for the adverse effect of TCP phase on the stress rupture life. The TCP phase is the site for crack initiation, which is the easy way for crack propagation in stress rupture process because of its brittle nature[39]. The TCP precipitates destroy the continuity of the microstructure. The solid solution strengthening elements, such as W and Re, are enriched in the TCP phase, as shown in Table 2, which leads to poor Re and W in the matrix surrounding the TCP phase and reduces the solid solution strengthening effect of the γ matrix.

Therefore, it can be deduced reasonably that the degeneration of stress rupture life with increase in Re content is dominated by significant increase in TCP phase formation.

4 Conclusions

1) The size of γ' phase decreases, and the volume fraction

and cubic degree of γ' phase slightly increase with increase in Re content of the fourth generation single crystal superalloy DD15. In the long term aging, the γ' phase coarsens, and drafting rate, the precipitate rate and volume fraction of TCP phase are all improved with increase in Re content. The microstructure stability of the alloy declines with increase in Re content.

2) The stress rupture life of the alloy declines significantly with increase in Re content. The three ruptured specimens all exhibit the presence of TCP phase. The amount of TCP phases increases greatly with increasing Re content. TCP phase can be the site of crack initiation. This is the main reason for the decrease in stress rupture life of the alloy with increase in Re content.

3) The dislocation networks formed at the γ/γ' interface of ruptured specimen turn denser with increase in Re content. Re has a strong segregation tendency in γ matrix. The partition ratio of Re rises significantly with increase in Re content. The lattice misfit of the alloy turns larger toward negative with increase in Re content.

References

1 Walston S, Cetel A, Mackay R *et al. Superalloys 2004*[C]. Pennsylvania: TMS, 2004: 15

2 Caron P, Khan T. *Aerospace Science and Technology*[J], 1999, 3: 513

3 Ming H, Jing Z. *Rare Metals*[J], 2016, 35(2): 127

4 Rüsing J, Wanderka N, Czubayko U *et al. Scripta Materialia*[J], 2002, 46: 235

5 Pandey P, Sawant A K, Nithin B *et al. Acta Materialia*[J], 2019, 168: 37

6 Blavette D, Caron P, Khan T. *Scripta Metallurgical Materials* [J], 1986, 20: 1395

7 Epishin A, Bückner U, Portella P D *et al. Scripta Materialia*[J], 2003, 48: 455

8 Zeng Q, Ma S W, Zheng Y R *et al. Journal of Alloys and Compounds*[J], 2009, 480(2): 987

9 Giamei A F, Anton D L. *Metallurgical Transaction*[J], 1985, 16: 1997

10 Wang W Z, Jin T, Liu J L *et al. Materials Science and Engineering A*[J], 2008, 479: 148

11 Tian S G, Zeng Z, Liang F S *et al. Materials Science and Engineering A*[J], 2012, 543: 104

12 Huang M, Cheng Z Y, Xiong J C *et al. Acta Materialia*[J], 2014, 76: 294

13 Ge B H, Luo Y S, Li J R *et al. Scripta Materialia*[J], 2010, 63(10): 969

14 Ding Q Q, Li S Z, Chen L Q *et al. Acta Materialia*[J], 2018, 154: 137

15 Zhu T, Wang C Y, Gan Y. *Acta Materialia*[J], 2010, 58(6): 2045

16 Li J R, Tang D Z, Lao R L *et al. Journal of Materials Science and Technology*[J], 1999, 15(1): 53

17 Erickson G L. *Superalloys 1996*[C]. Pennsylvania: TMS, 1996: 35

18 Tian S G, Zeng Z, Liang F S *et al. Materials Science and Engineering A*[J], 2012, 543: 104

19 Luo Y S, Li J R, Liu S Z *et al. Journal of Materials Engineering*[J], 2005(8): 10 (in Chinese)

20 Chang J X, Wang D, Dong J S *et al. Chinese Journal of Materials Research*[J], 2017, 31(9): 695 (in Chinese)

21 Pu S, Xie Guang, Wang Li *et al. Acta Metallurgica Sinica*[J], 2016, 52(5): 538 (in Chinese)

22 Hu T W, Lu J, Xu Y *et al. Acta Metallurgica Sinica*[J], 2019, 55(11): 1427

23 Acharya M V, Fuchs G E. *Materials Science and Engineering A*[J], 2004, 381: 143

24 Yan H J, Tian S G, Zhao G Q *et al. Materials Science and Engineering A*[J], 2019, 768: 138 437

25 Wang X G, Liu J L, Jin T *et al. Materials and Design*[J], 2015, 67: 543

26 Heckl A, Rettig R, Singer R F. *Metallurgical and Materials Transactions A*[J], 2010, 41(1): 202

27 Mottura A, Miller M, Reed R. *Superalloys 2004*[C]. Pennsylvania: TMS, 2004: 891

28 Shi Z X, Liu S Z, Li J R *et al. Journal of Materials Engineering*[J], 2019, 47(5): 107 (in Chinese)

29 Shi Z X, Liu S Z, Yue X D *et al. Rare Metal Materials and Engineering*[J], 2022, 51(10): 3542

30 Zhang J X, Murakumo T, Koizumi Y *et al. Metallurgical and Materials Transactions A*[J], 2002, 33: 3741

31 Argence D, Vernault C, Desvallees Y *et al. Superalloys 2000*[C]. Warrendale: TMS, 2000: 829

32 Maciej Z, Steffen N, Mathias G *et al. Metal and Materials International*[J], 2017, 23(1): 126

33 Tian S G, Zhang B S, Shu D L *et al. Materials Science and Engineering A*[J], 2015, 643: 119

34 Han Y F, Ma W Y, Dong Z Q *et al. Superalloys 2008*[C]. Pennsylvania: TMS, 2008: 91

35 Wang T, Sheng G, Liu Z K *et al. Acta Materialia*[J], 2008, 56(19): 5544

36 Chen J Y, Feng Q, Chao L M *et al. Progress in Natural Science: Materials International*[J], 2010, 20: 61

37 Pyczak F, Devrient B, Neuner F C *et al. Acta Materialia*[J], 2005, 53(14): 3879

38 Zhang J X, Murakumo T, Harada H *et al. Scripta Materialia*[J], 2003, 48(3): 287

39 Shi Z X, Li J R, Liu S Z. *Progress in Natural Science: Materials International*[J], 2012, 22(5): 426

Re含量对DD15单晶高温合金显微组织和持久性能的影响

史振学，刘世忠，岳晓岱，王志成，李嘉荣
(北京航空材料研究院 先进高温结构材料重点实验室，北京 100095)

摘　要：在定向凝固炉中制备了3种不同Re含量（5%，6%，7%，质量分数）、其它合金元素相同的第4代单晶高温合金DD15，将其完全热处理后在1100 ℃长期时效1000 h，在1100 ℃/137 MPa条件下测试合金的持久性能。研究了Re含量对DD15单晶高温合金组织稳定性和持久性能的影响。结果表明，随着Re含量增加，γ'相尺寸减小，其体积分数和立方化程度稍有增加，长期时效时γ'相粗化、筏排化速率和TCP相析出量增加，合金的组织稳定性降低。合金的持久性能随着Re含量增加而显著降低。3种断裂试样中均发现了TCP相，其含量随着Re含量增加而增多，这是合金持久性能随Re含量增加而降低的主要原因。γ/γ'相界面位错网密度随着Re含量增加而增加。Re元素在γ基体中有强烈的偏析倾向，分配比随Re含量增加而显著升高。随着Re含量增加，合金的晶格错配度向负方向增加。

关键词：单晶高温合金；DD15；Re含量；持久性能

作者简介：史振学，男，1975年生，博士，研究员，北京航空材料研究院先进高温结构材料重点实验室，北京 100095，电话：010-62498312，E-mail：zhenxue.shi@biam.ac.cn